JOURNAL OF GEOPHYSICAL RESEARCH, VOL. 106, NO. A12, PAGES 29,355–29,362, DECEMBER 1, 2001

Evidence for charge drift modulation at intermediate solar activity from the flux variation of protons and α particles

G. Boella and M. Gervasi

Istituto Nazionale di Fisica Nucleare – Sezione di Milano, Milan, Italy
Physics Department, University of Milano-Bicocca, Milan, Italy

S. Mariani and P.G. Rancoita

Istituto Nazionale di Fisica Nucleare – Sezione di Milano, Milan, Italy

I. G. Usoskin

Istituto Nazionale di Fisica Nucleare – Sezione di Milano, Milan, Italy
Sodankyla Geophysical Observatory, University of Oulu, Oulu, Finland

Abstract. We have studied the flux of galactic protons and helium nuclei measured at 1 AU along two consecutive solar activity cycles. We have correlated cosmic ray fluxes measured on IMP 3 satellite at low energy (50 - 300 MeV amu^{-1}) with neutron monitor counts registered at Climax station (at energies above few GeV) during the period 1973 - 1995. We have found a systematic excess in the flux of the positive charged particles during the periods with positive solar magnetic field polarity ($A > 0$) with respect to the flux during the periods of negative polarity ($A < 0$). This flux excess gives an experimental evidence that charge drift effect plays an important role in the modulation of galactic cosmic rays. A systematic investigation of charge drift modulation is presented. The dependence of the drift effect on the solar activity phase and the particle energy has been also studied. A variation of the proton (as well as helium) flux might be as large as 40%, at the solar activity minimum of two contiguous cycles, at energy $\leq$ 100 MeV.

1. Introduction

The intensity and the spectrum of galactic cosmic rays (GCRs) entering the heliosphere are modified as they travel through the interplanetary magnetic field (IMF, indicated also as B) embedded in the solar wind in the heliospheric cavity. The propagation of GCRs in the heliosphere is described by the transport equation, as discussed in section 2. Observational data, as well as theoretical models, suggest that part of the modulation in the solar cavity is charge sign dependent. Drift is one of the long-term leading mechanisms in solar modulation of GCRs, and its effect is dependent on the charge sign of particles interacting with the IMF.

In a series of papers [*Kota and Jokipii*, 1983; *Jokipii and Thomas*, 1981; *Jokipii and Davila*, 1981] the theory of drift motion has been developed. Numerical modulation models including drift effect have produced flux predictions in good agreement with observations over a complete solar cycle [*Potgieter and Moraal*, 1985; *Reinecke et al.*, 1997]. These models have shown that drift effects play an important role in modulation, in particular, during periods of solar minimum. Even better results have been obtained developing time-dependent models of solar modulation [*LeRoux and Potgieter*, 1995], but the actual influence of the drift mechanism has not been established yet.

Paper number 2001JA900075.
0148-0227/01/2001JA900075$09.00

We have developed a method to evaluate drift efficiency for 0.4 - 1.5 GV GCRs for different levels of solar activity. We used data taken by Climax neutron monitor (NM) and on board IMP 8 satellite. Data cover 25 years (see section 3), strictly needed to investigate a duration longer than two solar cycles, and allow the long-term analysis. At NM energies, particle propagation is slightly affected by drift motion. Therefore NM counting rate can be mostly associated with the diffusion modulation conditions of the heliosphere, while only minor effects can be ascribed to the drift motion [*Clem et al.*, 1996]. On the other hand, at satellite detectable energies, outside the magnetosphere, drift motion deeply influences GCRs' flux. Fluxes of low-energy particles in periods with opposite magnetic polarity differs from each other even if the NM counting rate is the same. The ratio of the flux values can be assumed as directly connected to drift mechanism efficiency. In section 5 it has been found to be different for different levels of NM counting rate and for different particle energies.

2. Role of Drift in the GCRs Propagation

2.1. Transport Equation

The transport equation of GCRs in the solar cavity is written in general terms as follows [*Parker*, 1965]:

$$\frac{\partial f}{\partial t} = -(V + < v_d >) \cdot \nabla f + \nabla \cdot (K^{(s)} \cdot \nabla f) + \frac{1}{3}(\nabla \cdot V)\frac{\partial f}{\partial \ln P}, \quad (1)$$

where $f(r,P,t)$ is the omnidirectional distribution function of

GCRs, P is rigidity, r is distance from the Sun, t is time, and V is the solar wind velocity. K denotes the diffusion tensor, which can be divided into a symmetric part $K^{(s)}$ and an antisymmetric part $K^{(a)}$. The symmetric part relates to diffusion, and the antisymmetric part describes the gradient and curvature drifts. The vector

$$< v_d >= \nabla \times K^{(a)} \cdot \frac{\vec{B}}{B} \qquad (2)$$

is the pitch angle averaged guiding center drift velocity. The first term on the right-hand side of (1) includes the outward convection of GCRs due to the solar wind and the GCRs particle drift due to curvature and gradient of the IMF. The second term describes the inward diffusion, and the third term describes the adiabatic energy loss. In the coordinate system determined by IMF the diffusion tensor can be written in the form

$$K = \begin{vmatrix} k_{\parallel} & 0 & 0 \\ 0 & k_{\perp} & k_T \\ 0 & k_T & k_{\perp} \end{vmatrix} = K^{(s)} + K^{(a)}. \qquad (3)$$

The symmetric part of the diffusion tensor includes the diffusion coefficients parallel ($k_{\parallel}$) and perpendicular ($k_{\perp}$) to the mean magnetic field. The antisymmetric term k_T represents the drift coefficient.

2.2. Charge Drift Effect

The main component of the heliospheric magnetic field B can be represented by the Parker spiral. The B vector has both gradient and curvature features. The flux of charged particles can be affected by IMF variations if the typical scale length is of the order or smaller than the corresponding particles' Larmour radius. The Larmour radius of the particle changes, and the guiding center of the motion translates, perpendicularly both to the field and the gradient. In the standard Parker spiral magnetic field the drift velocity (equation (2)) for charged particles with velocity βc and rigidity P takes the form [*Potgieter and Moraal*, 1985]

$$< v_d >= \frac{\beta P}{3} \nabla \times \left(\frac{\vec{B}}{B^2} \right). \qquad (4)$$

It is important to highlight that drift velocity has an opposite direction for opposite charged particles. This fact drives negative charged particles to follow a different path in the heliosphere respect to positive ones. On the other hand, the importance of drift for solar modulation in the Parker equation (1) is the product $v_d \cdot \nabla f$. While v_d is increasing with the particle energy, the effect of modulation is conversely decreasing, because ∇f is small at high energy.

Periods with positive heliomagnetic field polarity ($A > 0$) present magnetic field lines exiting from the northern solar hemisphere. During these phases, positive charged particles (p, e^+, and nuclei) have a higher probability of reaching the Earth coming from the polar regions of the heliosphere, while negative charged particles (e^- and $\bar{p}$) come mainly from the ecliptic regions along the heliospheric current sheet (HCS). The situation is reversed during solar cycles with negative magnetic field polarity ($A < 0$) [*Jokipii and Kopriva*, 1979; *Jokipii and Davila*, 1981]. In spite of the same solar modulation strength [*Gleeson and Axford*, 1968], the flux of particles propagating through the HCS undergoes a different solar modulation respect to the flux of particles coming from the polar regions of the heliosphere. Usually, the flux of particles propagating through the HCS undergoes a higher reduction [*Jokipii and Kopriva*, 1979].

Efficiency of charge drift effect is at maximum when solar activity is at minimum. It is related to the heliospheric current sheet tilt angle and therefore to the level of solar activity. Charge drift effect becomes ineffective at high values of solar modulation strength because of high waviness of HCS [*Burlaga et al.*, 1984; *Potgieter et al.*, 1993a]. Drift motion affects cosmic rays up to neutron monitor energies. Effects on modulated spectra can be relevant for particles with rigidities, P, as large as 4 GV [*Bieber and Matthaeus*, 1997]. In fact, the proton spectrum measured during a $A > 0$ solar minimum is considerably higher than what is found during a $A < 0$ solar minimum, especially for rigidity $P < 1$ GV. A difference up to ~ 30% in the flux has been reported at a kinetic energy of ~ 200 MeV [see *Garcia-Munoz et al.*, 1986, Figure 11].

In the present paper we assume that the difference between $A > 0$ and $A < 0$ periods is only due to the drift effect. However, the alteration of the IMF polarity might also affect other modulation parameters, for example, the perpendicular diffusion ($k_{\perp}$) [*Potgieter*, 2000]. Therefore the results we have found can be considered as an upper limit of the drift effect, while they take into account the full charge sign dependence of the GCRs solar modulation.

3. Data Description

3.1. IMP 8

The IMP 8 satellite was launched on October 26, 1973, to measure the interplanetary magnetic field, solar plasma, and energetic charged particles at 1 AU (for more information, see the IMP 8 Web page: http://nssdc.gsfc.nasa.gov/space/). It is still operating in its near-circular, 35 Earth radii, 12-day revolution orbit. The goals of the extended IMP 8 mission were to provide a 1-AU baseline for deep space studies and to monitor continuously solar cycle variations by means of a single set of well-calibrated and well-understood instruments.

The medium energy detector (MED), one of the instruments on board the satellite, has been detecting mainly protons and α particles. The detector system is a three-element telescope: the middle element is a *CsI* scintillator, while the other two elements are solid state sensors. The acceptance of the system is a few cm^2 sr, and depends on the particles energy. Drifts in the long-term gain of the photomultipliers have been corrected during data reduction through an analysis of the minimum ionizing peak signal position (see the Web page: http://spdf.gsfc.nasa.gov/imp8_GME/GME_instrument.html).

We have used six channels of MED as shown in Table 1. Two channels have detected protons, while the remaining four have measured α particles. Here IMP 8 flux is given in counts s^{-1} cm^{-2} sr^{-1} (GeV/amu)$^{-1}$. We have also considered one more

Table 1. Channels of MED[a] Used in This Data Analysis[b].

Channel	Energy Band, MeV amu^{-1}	Particles
P1	28.74 - 63.20	p
P2	121.0 - 229.5	p
A2	81.0 - 101.0	α
A3	134.5 - 168.8	α
A4	168.8 - 198.5	α
A5	168.8 - 381.5	α

[a]MED, medium energy detector.
[b]In the last column the particle identity has been reported.

channel of α particles at lower energy (channel A1 in the range 28.6 - 63.3 MeV amu^{-1} of kinetic energy), but we have excluded it from the analysis because of a significant contamination by anomalous cosmic rays.

3.2. Climax Neutron Monitor

The Climax NM is operated in Colorado at an altitude of 3600 m above see level (asl). It detects mainly secondary neutrons, coming from the interaction in the atmosphere of primary protons and helium of GCRs (see the Climax neutron monitor Web page: http://odysseus.uchicago.edu/NeutronMonitor/). The geomagnetic cutoff rigidity of the station is ~ 3 GV.

The absolute counting rate accuracy of the Climax NM is of the order of 1% (for details, see the Climax neutron monitor Web page). The main sources of uncertainty are given by pressure corrections and periodical intercalibration after substitution of aged parts of the detector. Because of large number counts, the statistical error is negligible. In this paper the NM counting rate value, expressed in counts s^{-1}, is rescaled by a factor of 200.

Climax NM counts, recorded during several solar activity minimum periods, present variations of only ~ 2% [*Reinecke and Potgieter*, 1994]. These measurements confirm the long-term stability of the NM counts. Furthermore, these variations (2%) have to be considered as an upper limit to the contribution of the charge drift effect.

We have estimated the effect of drift modulation on the Climax NM counts independently. We have performed a Monte Carlo simulation using the model by *Debrunner and Fluckiger* [1983], propagating cosmic rays from the top of the atmosphere to the NM detector (on the ground) and then using a standard NM response function. This way we get the yield function, i.e., the NM counts per primary cosmic ray, for the several components of the GCRs as a function of the kinetic energy. We have used modulated proton spectra from *Boella et al.* [1998], while using abundances for He, C, and Fe, relative to protons from *Longair* [1992]. Here are a few remarkable results:

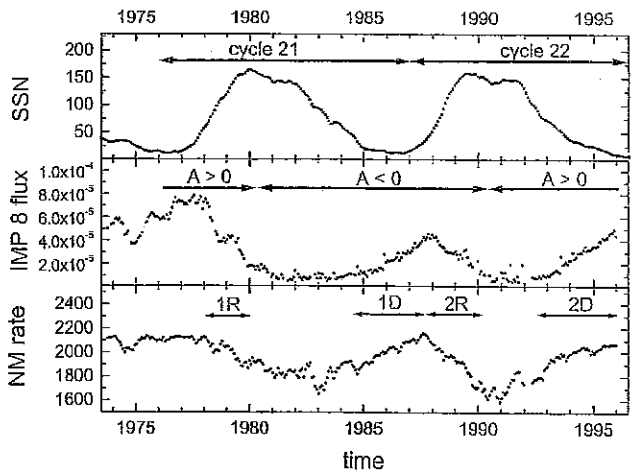

Figure 1. (top) Time profile of solar activity according to the smoothed sunspot number (SSN), (middle) Time profile of lower-energy cosmic protons as measured by IMP 8, P1 channel (in counts s^{-1} cm^{-2} sr^{-1} (GeV/amu)$^{-1}$), (bottom) Time profile of cosmic rays as measured by Climax neutron monitor (NM), in counts s^{-1}/200. Solar cycles covered by the data are shown in the top panel. IMF polarity is shown in the middle panel. Time intervals selected for data analysis are highlighted in the bottom panel (for details, see the text and Table 2).

Table 2. Time Intervals Selected for the Analysis[a].

Period	Time Interval[b]	Solar Cycle	IMF Polarity	Solar Phase
1R	12/77 - 4/80	21	+	Rising
1D	5/84 - 9/87	21	-	Declining
2R	9/87 - 2/90	22	-	Rising
2D	6/92 - 12/95	22	+	Declining

[a]The labels used in Figure 1 are reported in the first column.
[b]Format of time intervals is: month/year.

1. The Climax NM counting rate is mostly related to the proton primary component (~ 70-75%), depending on the solar modulation strength. The helium component contributes ~ 25-20%, while heavier elements account only for less than 5%. It is important to remember that α particles and heavier elements are modulated less compared to the proton component.

2. Climax NM is sensitive to primary protons with kinetic energy above the threshold of 2 GeV. However, actually, the major contribution to the NM counts comes from primary cosmic rays with higher energy (~ 10 GeV). Furthermore, cosmic rays contribute up to ~ 100 GeV, in spite of the quickly decreasing spectrum.

3. Primary protons in the interval 20 - 100 GeV contribute to Climax NM counts for ~ 30%. At these energies, protons are almost nonmodulated. If we consider the contribution of α particles and heavier nuclei, the NM fraction nonmodulated increases up to ~50%.

4. Primary protons in the interval 4 - 20 GeV contribute to Climax NM counts for 35-42%, depending on the solar activity. This part is modulated; however, these protons are not affected significantly by the drift effect [*Reinecke and Potgieter*, 1994].

5. Primary protons in the interval 2 - 4 GeV contribute to Climax NM counts for less than 3%. This part is both modulated and sensitive to the drift effect.

We estimate an upper limit of 10% to the primary flux variation due to the charge drift effect at 2 GeV and even less at higher energy [see also *Garcia-Munoz et al.*, 1986; *Reinecke and Potgieter*, 1994; *Boella et al.*, 1998]. Besides, at energy higher than 4 - 5 GeV, no charge drift modulation is expected. As a consequence of that discussed above, the overall variation cannot affect the NM counts by more than 1%.

4. Data Analysis

We have compared the flux of low-energy GCRs collected on board IMP 8 satellite during periods belonging to consecutive solar cycles and having the same recorded NM counting rates. These fluxes came from periods of opposite solar magnetic field polarity. Assuming a constant flux of GCRs entering the solar cavity, rate differences should be attributed to the drift mechanism. This procedure has been followed to investigate the solar drift modulation of the positronic fraction previously [*Clem et al.*, 1996].

The time profile shown in Figure 1 presents data of solar cycles 21 and 22: We have compared separately rising and declining phases of solar activity. It is well known that solar modulation dynamics is not the same during the two phases. In fact, cosmic ray flux is influenced by the heliospheric

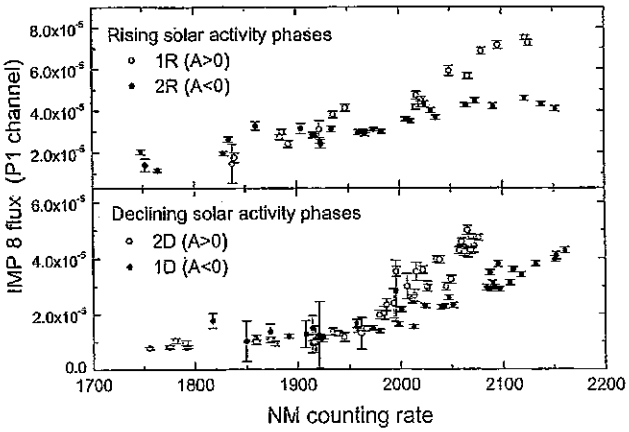

Figure 2. IMP 8 P1 channel flux versus NM counting rates taken during (top) the rising phase of two consecutive solar cycles and (bottom) the declining phase of two consecutive solar cycles. Open circles are data from cycles with $A > 0$, and solid circles from cycles with $A < 0$.

conditions that occurred in the previous months [*Dorman and Dorman*, 1967; *Usoskin et al.*, 1998].

The drift effect can be important during periods of weak and intermediate solar activity (see, e.g., review by *Fisk et al.*, [1998]). Therefore we have limited our analysis to these solar activity periods. The time intervals we have selected for the analysis are shown in Figure 1 and described in Table 2. We have also verified that during periods of high solar activity there is no evidence of charge sign drift effect (i.e., we have found that the ratio R, as defined in the following discussion, is consistent with the value 1).

We have removed data recorded during periods with strong solar events and Forbush decreases, since these are short-term phenomena not related to the drift effects. In Figure 2, data taken during both rising and declining phases of the solar activity have been represented after the preanalysis selection described above.

Some hysteresis loop is also evident in the correlation profiles of IMP 8 versus NM rates. Loops are due to the time delay of low-energy GCRs with respect to high-energy ones

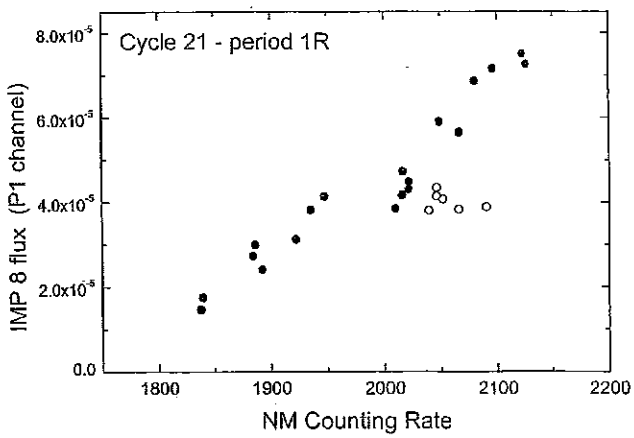

Figure 3. P1 channel flux versus NM counting rate for data recorded during the rising phase of the solar cycle 21 (period 1R in Table 2). Data labeled with open circles have been rejected from the analysis.

when reacting to changing modulation conditions. Most of these loops do not modify the general trend of the data. We have rejected, in all the analyzed channels, data recorded during one particular larger hysteresis loop. This loop has occurred in the rising phase of the solar cycle 21 (August 1978 to February 1979). We have rejected data placed clearly outside the general trend of the data preceding and following this period. An example of the loop data rejection is shown in Figure 3.

Let us introduce the parameter R to estimate the drift effect. R is the ratio among IMP 8 fluxes Φ measured in solar cycles with opposite polarity for the same value of NM counting rate:

$$R(NM) = \frac{\Phi^{-}(NM)}{\Phi^{+}(NM)}, \qquad (5)$$

where the fluxes $\Phi^{-} = \Phi_{A<0}$ and $\Phi^{+} = \Phi_{A>0}$ are measured by the same channel of IMP 8, and therefore for the same range of energy. No drift effect means $\Phi^{-}(NM) \cong \Phi^{+}(NM)$ or $R(NM)$ consistent with 1.

Original data are 26-day averages (over a single solar Bartel rotation). These points are oversampling the time interval we are interested in to highlight the long-term effect. In fact, short-term changes in modulation are evident. Therefore we have binned data in six groups with respect to the NM counting rate. The number of points per bin has been chosen in order to reduce the statistical fluctuation and to avoid large systematic effects inside a single bin. Moreover, corresponding intervals must be similar in $A > 0$ and $A < 0$ periods for each energy channel in order to compute the ratio R. Selected bin intervals are shown in Table 3.

We have considered two sources of error: (1) the intrinsic dispersion of the data inside a single bin and (2) the variation of the average with respect to different choices of the bin intervals. We have moved the bins boundaries (approximately $\pm$ 20 NM units around the values reported in Table 3) in order to fluctuate the average value. This additional uncertainty, as well as the variation of the average value, has been taken into account when the final average and error bars have been computed.

As discussed in section 3, the charge drift modulation could be a source of systematic error in the NM counting rate. However, the effect is lower than 2%. This systematic uncertainty in the NM counts is taken into account by the procedure of the variation of the bins' boundaries, described above.

5. Results

5.1. Ratio R for the Different Channels

The plots of R as a function of NM are shown in Figure 4 for rising and declining solar phases. As shown in Figure 4, the values of R for the lowest-energy channels with high NM

Table 3. Selected Bin Intervals in Climax Neutron Monitor Counting Rate.

Bin Number	Rate Interval, counts s^{-1}/200
NM1	1825 - 1920
NM2	1920 - 1975
NM3	1975 - 2013
NM4	2013 - 2042
NM5	2042 - 2080
NM6	2080 - 2118

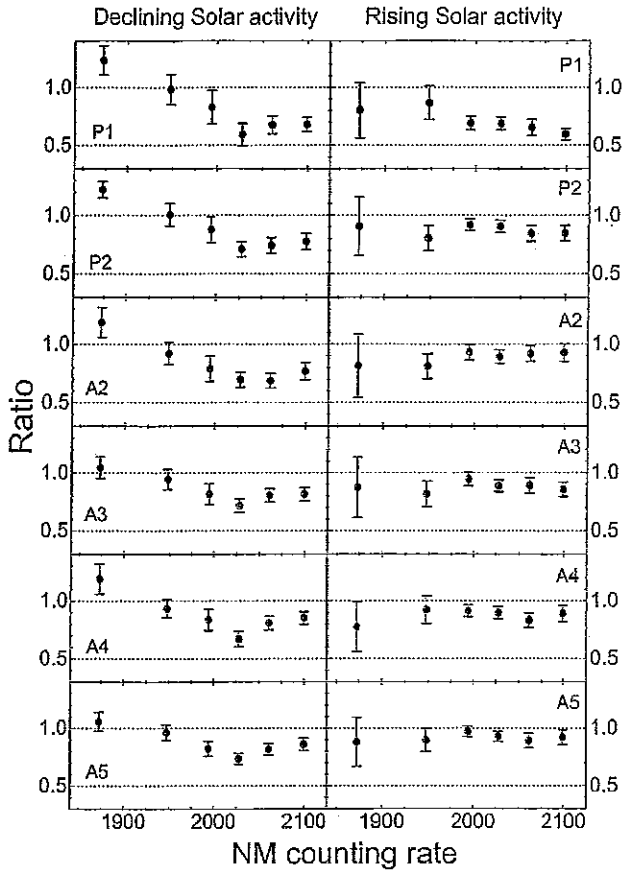

Figure 4. Ratio R versus the neutron monitor counting rate. Different panels correspond to different IMP 8 channels (rows) and to different solar activity phases (columns).

rates are lower than 1. As qualitatively expected, drift models predicts that the charge drift is reduced with rising solar activity and rising energy (for instance, see *Potgieter et al.* [1993b]). The data shown in Figure 4 are in agreement with such a prediction: The higher the NM rate is, the more R decreases. Besides, the same trend is found moving from high- to low-energy channels.

Data show a different behavior during declining and rising solar activity phases. Data from declining solar phases show a more evident effect: All the channels seem to be affected by charge drift effect at low solar activity. Data from rising solar activity show a clear effect for channels P1 and P2 but a marginal depletion of R for the α particle channels. This difference can be due to different phenomena like an hysteresis effect. The same level of NM count rate corresponds to slightly different levels of solar activity and hence to a different drift effect for rising and declining phases of solar cycle. Our results confirm that the relations between diffusive and drift terms in the modulation change over the solar cycle. In other words, there is a kind of hysteresis in drift versus diffusion.

At low counting rate values of the neutron monitor (i.e., at medium and high solar activity), data appear noisy, as can be expected in a turbulent heliosphere. Anyway, at a low NM counting rate, data stay around the value $R = 1$. This is a confirmation that no effect is found for any energy, and no general behavior can be inferred in those situations. Data for

Table 4a. Null Hypothesis Test[a].

IMP 8 Channel	Declining Phase	Rising Phase
P1	< 0.1	< 0.1
P2	< 0.1	0.5
A2	< 0.1	11
A3	< 0.1	1.0
A4	< 0.1	0.8
A5	< 0.1	18

[a]Values of the ratio R have been fitted with a constant $R = 1$. Here the χ^2 probability (in percent) to exceed the found value is reported. Fitting function has to be rejected when the probability reported is lower than a threshold value. Values refer to the different channels of Figure 4.

the highest solar activity (NM1 and NM2) show no systematic deviation from R consistent with 1. This evidence confirms that there is no offset in the data (and in the analysis). Therefore the values $R < 1$ found at weaker solar activity seem to be due to a real charge sign modulation, while we are not able to disentangle the drift effect from the other modulation parameters affected by IMF polarity variation.

Plots of declining solar activity show a minimum at NM4 in all the channels. This feature is probably connected with some disturbance in the heliosphere that occurred during cycle 21 or 22 at this value of the NM counting rate. On the other hand, the trend of R looks similar throughout all the channels in the same solar phase. This is an indication that

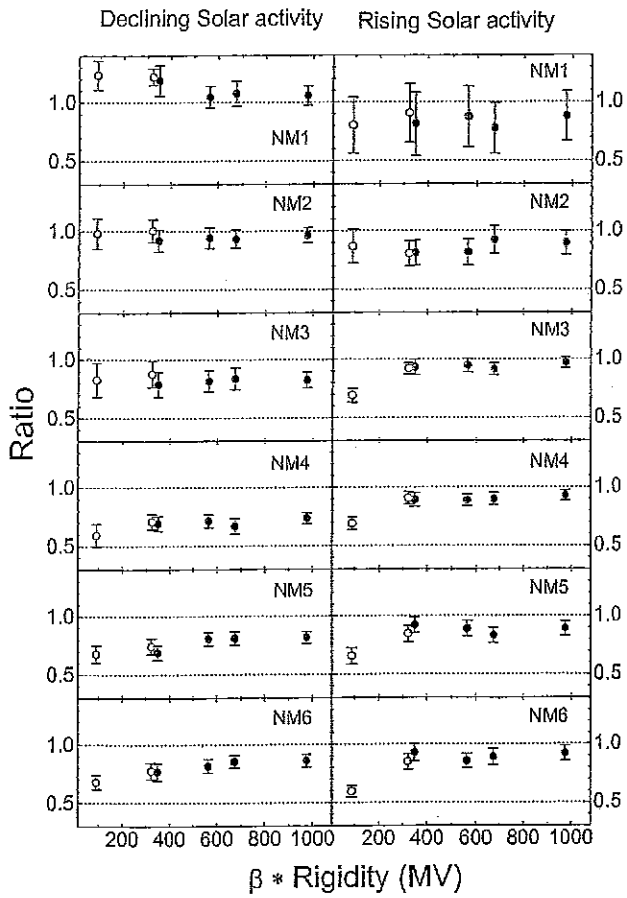

Figure 5. Ratio R versus βP. Different panels correspond to different NM bins (rows) and to different solar activity phases (columns). Open circles are proton channels; solid circles are α channels.

Table 4b. Null Hypothesis Test[a].

NM Bin	Declining Phase	Rising Phase
NM1	1.2	82
NM2	90	7
NM3	0.3	< 0.1
NM4	< 0.1	< 0.1
NM5	< 0.1	< 0.1
NM6	< 0.1	< 0.1

[a]See the comments in Table 4a. Values refer to the different bin numbers of Figure 5.

short-term energy-dependent disturbances and hysteresis loops do not play a major role.

As described in section 4, we have removed data showing a larger loop feature during the rising phase of cycle 21. These data have been rejected from the bins NM3 to NM5. Values of R for these bins do not show a particular behavior with respect to the other bins. On the other hand, data that survived the rejection show a residual suppression of the drift effect (see Figures 2 and 3).

We have used a statistical method to evaluate these plots. We have tested the hypothesis that data are fitted by the constant $R = 1$ (i.e., a null hypothesis test). Results are reported in Table 4a. The difference among rising and declining phases is highlighted: During a declining phase the effect is confirmed for all the channels; during a rising phase the effect is clear for the proton channels but marginal for the α particles. Also, the disappearing of the effect at high solar activity is confirmed.

5.2. Ratio R for the Different NM Bins

In addition, βP seems to be a better suited parameter to describe the dependence of R for both protons and α particles than the rigidity P alone or the kinetic energy E_k. This is in agreement with (4), where the same drift speed v_d is found for particles with the same βP. The parameter βP seems to describe better the dependence of R at the solar activity minimum, when charge drift is effective. Plots of R as a function of βP are shown in Figure 5.

In general, data show different behaviors in rising and declining phases. The effect seems to be larger in the latter

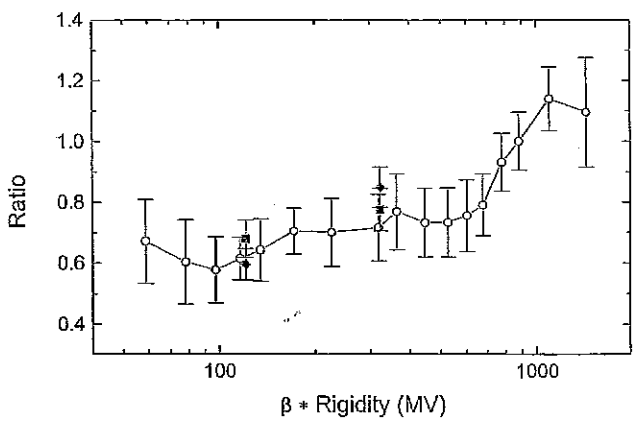

Figure 6. Ratio R versus βP for protons at the minimum solar activity. Open symbols are data from *Garcia-Munoz et al.* [1986]; solid symbols are data from IMP 8 (channels P1 and P2) for the bin NM6 (solid square is for declining solar activity, and solid diamond is for rising solar activity).

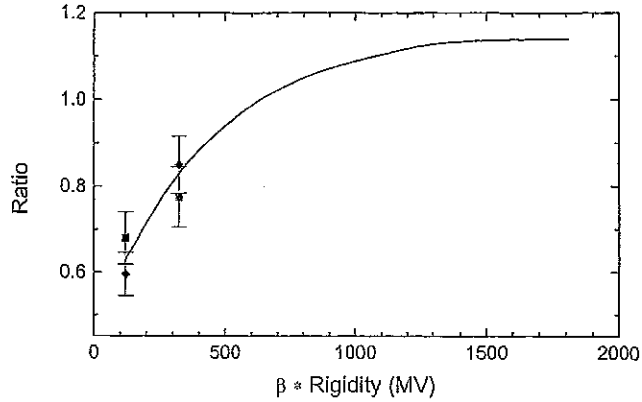

Figure 7. Ratio R versus βP for protons at the minimum solar activity. The solid line is the model from *Reinecke et al.* [1997]; solid symbols are the same as those plotted in Figure 6.

one, and at low solar activity, R is well below 1 for all the channels. In rising phases the effect is evident only for $\beta P <$ 400 MV (i.e., for proton channels). Probably, while the solar activity is declining and going toward a solar minimum, the heliosphere reaches a situation of high drift efficiency, caused by the progressive disappearing of disturbing barrier phenomena, such as global merged interaction regions (GMIRs) [*Reinecke et al.*, 1997].

Here is still more evidence that at a low NM counting rate, data show a large error bar and stay around the value $R = 1$. We have used the same statistical method to evaluate these plots. Results are reported in Table 4b. A clear charge drift effect is confirmed for data belonging to bins NM3 to NM6 (at low solar activity), while no effect is found at a medium solar activity level (NM1 and NM2).

6. Discussion: Drift Effect at the Solar Minimum

6.1. Comparison With Previous Results

A comparison between present and published results has been carried out, although there is no study based on experimental data outside the solar activity minimum. In particular, flux of protons measured at solar activity minimum during cycles with opposite solar magnetic field polarity have been already studied by *Garcia-Munoz et al.* [1986]. In Figure 6 we compare data of IMP 8 (channels P1 and P2) at the highest NM level with data reported by *Garcia-Munoz et al.* [1986]. A good agreement can be observed.

Recently, a drift model that reproduced simultaneously spectra of p and α during solar minima of two consecutive solar cycles has been developed by *Reinecke et al.* [1997]. The model predicts different shapes of the ratio R versus P for

Table 5. Estimated Variation of Proton or Helium Flux During Solar Minima With Opposite Solar Magnetic Field Polarity[a].

E_k, Mev amu^{-1}	p, Mev c^{-1}	$1 - R$, %
50	310	40 ± 10
100	445	25 ± 8
200	645	20 ± 7
300	810	14 ± 6

[a]See the text for the definition of the ratio R.

Table 6. Estimated Variation of the Antiproton/Proton Ratio During Solar Minima With Opposite Solar Magnetic Field Polarity[a].

E_k, Mev amu^{-1}	p, Mev c^{-1}	$1 - R_\rho$, %
50	310	65 ± 15
100	445	45 ± 11
200	645	35 ± 10
300	810	28 ± 8

[a]See the text for the definition of the ratio R_ρ.

protons and helium in GCRs. We have found an greement between their prediction and our results only for protons (see Figure 7).

6.2. Variation of p Flux and $\bar{p}/p$ Ratio

In Table 5 we report the parameter $1 - R = (\Phi^+ - \Phi^-)/\Phi^+$ at the solar minimum. As shown in Table 5, drift modulation can largely affect the particle flux. About 40% of the depletion in flux is observed at a kinetic energy of 50 MeV for consecutive solar cycles at minimum activity. Above 300 MeV the effect is below 10%.

These results can be used to estimate the drift effects in the modulation of the antiproton ($\bar{p}$) to proton ratio. The charge drift effect on $\bar{p}$ is opposite that on p during a solar cycle with the same magnetic field polarity. In particular, we can assume for the same value of NM count rate and energy (or rigidity):

$$R(NM)_{\bar{p}} = \frac{\Phi^+(NM)_{\bar{p}}}{\Phi^-(NM)_{\bar{p}}} \cong \frac{\Phi^-(NM)_p}{\Phi^+(NM)_p} = R(NM)_p . \qquad (6)$$

As a consequence, for the variation of the $\bar{p}/p$ ratio ($\rho = \Phi_{\bar{p}}/\Phi_p$), going from a cycle with $A < 0$ to a cycle with $A > 0$, we find

$$R_\rho = \frac{\rho^+}{\rho^-} = \frac{\Phi_{\bar{p}}{}^+}{\Phi_p{}^+}\frac{\Phi_p{}^-}{\Phi_{\bar{p}}{}^-} = \frac{\Phi_{\bar{p}}{}^+}{\Phi_{\bar{p}}{}^-}\frac{\Phi_p{}^-}{\Phi_p{}^+} \cong R^2(NM)_p . \qquad (7)$$

In fact, by reversing the polarity when the proton flux is decreasing, the antiproton one increases, producing an even larger variation. In Table 6 we give an evaluation of the expected relative variation of the ratio R_ρ. The assumption we have adopted (equation (6)) is a zero-order approximation, since the spectrum of protons is different from that of antiprotons [*Boella et al.*, 1998]. The estimated effect can be considered as an upper limit, especially in the low energy range.

7. Conclusions

In the present paper the charge drift effect has been investigated for both protons and helium nuclei. We have analyzed data covering more than two complete solar cycles with opposite magnetic field polarity, looking at the long-term variations in the heliosphere.

The effect is evident for low-energy GCRs measured at the solar activity minimum. The results obtained are in agreement both with models' predictions [*Reinecke et al.*, 1997] and previous results [*Garcia-Munoz et al.*, 1986]. The charge drift modulation becomes less effective going toward higher energy.

While at solar minima data have been already reported, we have extended the analysis out of the solar minimum, where drift effects become weaker with rising solar activity and there are no reliable models. The intensity of the effect is related to the decrease of the solar activity. We have found that drift modulation is still present up to a medium solar activity level especially in the lowest-energy channels. A difference among declining and rising solar activity phases is also found.

Finally, we have extrapolated our analysis to the $\bar{p}/p$ ratio. For this ratio a larger variation occurs, owing to the combination of this effect over the fluxes of the two populations. The variation among two solar minima with opposite field polarities can be as large as 60% for kinetic energy ~ 50 MeV amu^{-1}.

Acknowledgments. We would like to acknowledge F. McDonald, who provided us with the data of IMP 8 satellite, and the University of Chicago, National Science Foundation grant ATM-9613963, for the Climax neutron monitor data. Special thanks go to C. Paizis and to M. Storini for helpful discussions and fruitful suggestions. Referees' suggestions made an important contribution to improve substantially the paper.

Michel Blanc thanks both referees for their assistance in evaluating this paper.

References

Bieber, J.W., and W.H. Matthaeus, Perpendicular diffusion and drift at the intermediate cosmic-ray energies, *Astrophys. J., 485*, 655, 1997.

Boella, G., M. Gervasi, M.A.C. Potenza, P.G. Rancoita, and I. Usoskin, Modulated antiproton fluxes for interstellar production models, *Astropart. Phys., 9*, 261, 1998.

Burlaga, L.F., F.B. McDonald, N.F. Ness, R. Schwenn, A.J. Lazarus, and F. Mariani, Interplanetary flow systems associated with cosmic ray modulation in 1977-1980, *J. Geophys. Res., 89*, 6579, 1984.

Clem, J.M., D.P. Clements, J. Esposito, P. Evenson, D. Huber, and J. L'Heureux, Solar modulation of cosmic electrons, *Astrophys. J., 464*, 507, 1996.

Debrunner, H., and E.O. Fluckiger, Zu den solaren kosmischen strahlungseregnissen vom 15/11/1960, 22/11/1977 und 7/5/1978, Lizentiatsarbeit von Hans Christian Neuenschwander Physik. Inst. der Univ. Bern, Bern, Switzerland, 1983.

Dorman, I.V., and L.I. Dorman, Solar wind properties obtained from the study of the 11-year cosmic ray cycle, *J. Geophys. Res., 72*, 1513, 1967.

Fisk, L.A., J.R. Jokipii, G.M. Simnett, R. von Steiger, and K.P. Wenzel (Eds.), Cosmic rays in the heliosphere, *Space Sci. Rev., 83*(1/2), 1998.

Garcia-Munoz, M., P. Meyer, K.R. Pyle, J.A. Simpson, and P. Evenson, The dependence of solar modulation on the sign of the cosmic ray particle charge, *J. Geophys. Res., 91*, 2858, 1986.

Gleeson, L.J., and W.I. Axford, Solar modulation of galactic cosmic rays, *Astrophys. J., 154*, 1011, 1968.

Jokipii, J.R., and J.M. Davila, Effects of drift on the transport of cosmic rays, V, More realistic diffusion coefficients, *Astrophys. J., 248*, 1156, 1981.

Jokipii, J.R., and D.A. Kopriva, Effects of drift on the transport of cosmic rays, III, Numerical models of galactic cosmic-ray modulation, *Astrophys. J., 234*, 384, 1979.

Jokipii, J.R., and B. Thomas, Effects of drift on the transport of cosmic rays, IV, Modulation by a wavy interplanetary current sheet, *Astrophys. J., 243*, 1115, 1981.

Kota, J., and J.R. Jokipii, Effects of drift on the transport of cosmic rays, VI, A three-dimensional model including diffusion, *Astrophys. J., 265*, 573, 1983.

LeRoux, J.A., and M.S. Potgieter, A simulation of complete 11 and 22 year modulation cycles for cosmic rays in the heliosphere using a drift model with global merged interaction regions, *Astrophys. J., 442*, 847, 1995.

Longair, M.S., *High Energy Astrophysics*, Cambridge Univ. Press, New York, 1992.

Parker, E.N., The passage of energetic charged particles through interplanetary space, *Planet. Space Sci., 13*, 9, 1965.

Potgieter, M.S., Heliospheric modulation of cosmic ray protons: Role of enhanced perpendicular diffusion during periods of minimum solar modulation, *J. Geophys. Res., 105*, 18,295, 2000.

Potgieter, M.S., and H. Moraal, A drift model for the modulation of galactic cosmic rays, *Astrophys. J., 294*, 425, 1985.

Potgieter, M.S., L.A. Le Roux, L.F. Burlaga, and F.B. McDonald, The role of merged interaction regions and drifts in the heliospheric modulation of cosmic rays beyond 20 AU: A computer simulation, *Astrophys. J., 403*, 760, 1993a.

Potgieter, M.S., J.A. LeRoux, F.B. McDonald, and L.F. Burlaga, The causes of the 11-year and 22-year cycles in cosmic-ray modulation, *Proc. Int. Conf. Cosmic Rays 23rd, 3*, 525, 1993b.

Reinecke, J.P.L., and M.S. Potgieter, An explanation for the difference in cosmic ray modulation at low and neutron monitor energies during consecutive solar minimum periods, *J. Geophys. Res., 99*, 14,761, 1994.

Reinecke, J.P.L., H. Moraal, M.S. Potgieter, F.B. McDonald, and W.R. Webber, Different crossovers?, *Proc. Int. Conf. Cosmic Rays 25th, 2*, 49, 1997.

Usoskin, I.G., H. Kananen, G.A. Kovaltsov, K. Mursula, and P. Tanskanen, Correlative study of solar activity and cosmic ray intensity, *J. Geophys. Res., 103*, 9567, 1998.

G. Boella, and M. Gervasi, Physics Department, University of Milano-Bicocca, Piazza della Scienza 3, 20126 Milan, Italy. (massimo.gervasi@mib.infn.it)

S. Mariani, and P.G. Rancoita, INFN – Milano, c/o Physics Department, University of Milano-Bicocca, Piazza della Scienza 3, 20126 Milan, Italy. (piergiorgio.rancoita@mib.infn.it)

I.G. Usoskin, Sodankylä Geophysical Observatory, University of Oulu, P.O. box 3000, FIN-90014, Oulu, Finland.

(Received September 9, 2000; revised February 23, 2001; accepted April 23, 2001.)